Environmental Management (2014) 53:968–984
DOI 10.1007/s00267-014-0251-9

A Method for Spatially Explicit Representation of Sub-watershed Sediment Yield, Southern California, USA

Derek B. Booth · Glen Leverich · Peter W. Downs · Scott Dusterhoff · Sebastian Araya

Received: 4 January 2013 / Accepted: 11 February 2014 / Published online: 26 February 2014

Abstract We present here a method to integrate geologic, topographic, and land-cover data in a geographic information system to provide a fine-scale, spatially explicit prediction of sediment yield to support management applications. The method is fundamentally qualitative but can be quantified using preexisting sediment-yield data, where available, to verify predictions using other independent data sets. In the 674-km^2 Sespe Creek watershed of southern California, 30 unique "geomorphic landscape units" (GLUs, defined by relatively homogenous areas of geology, hillslope gradient, and land cover) provide a framework for discriminating relative rates of sediment yield across this landscape. Field observations define three broad groupings of GLUs that are well-associated with types, relative magnitudes, and rates of erosion processes. These relative rates were then quantified using sediment-removal data from nearby debris basins, which allow relatively low-precision but robust calculations of both local and whole-watershed sediment yields, based on the key assumption that minimal sediment storage throughout most of the watershed supports near-equivalency of long-term rates of hillslope sediment production and watershed sediment yield. The accuracy of these calculations can be independently assessed using geologically inferred uplift rates and integrated suspended sediment measurements from mainstem Sespe Creek, which indicate watershed-averaged erosion rates between about 0.6–1.0 mm year^{-1} and corresponding sediment yields of about 2 $\times$ 10^3 t km^{-2} year^{-1}. A spatially explicit representation of sediment production is particularly useful in a region where wildfires, rapid urban development, and the downstream delivery of upstream sediment loads are critical drivers of both geomorphic processes and land-use management.

Keywords Sediment yield · Wildfire · Urban development · GIS · Geomorphic landscape units · California

D. B. Booth (✉)
Bren School of Environmental Science & Management, University of California, Santa Barbara, CA 93106, USA
e-mail: dbooth@bren.ucsb.edu

D. B. Booth · G. Leverich · P. W. Downs · S. Dusterhoff · S. Araya
Stillwater Sciences, 2855 Telegraph Ave #400, Berkeley, CA 94705, USA

P. W. Downs
School of Geography, Earth and Environmental Sciences, Plymouth University, Plymouth PL4 8AA, UK

S. Dusterhoff
San Francisco Estuary Institute, 4911 Central Avenue, Richmond, CA 94804, USA

Introduction

Most of the attention given to watershed sediment yields by earth scientists has long focused on the quantification of these rates to inform our understanding of geomorphic processes and landscape denudation rates (e.g., Davis 1899; Gilbert 1904; Carson and Kirkby 1972; Dietrich and Dunne 1978; Selby 1982; Heimsath et al. 1997; Dietrich et al. 2003). Although the interplay of tectonic uplift, erosion, and landscape evolution is essential for studying the long-term development of the earth's surface, we suggest that simply characterizing the distribution and intensity of these processes has more immediate management applications, which include predicting threats to the ecological health of streams and lakes, the infilling of reservoirs, and the consequences of rapid stream-channel changes on adjacent human infrastructure (Dunne and Leopold 1978; Buffington et al. 2004; Downs and Gregory 2004; Downs and Booth 2011). Broad-scale estimates of landscape erosion and sediment production have been developed for many regions of the earth, based on long-term uplift rates, offshore sedimentation records, and cosmogenic dating of geomorphic surfaces (e.g., England and Molnar 1990; Milliman and Syvitski 1992; Reid and Dunne 1996; Granger and Riebe 2007). More local, short-term estimates have also been made using measured sediment loads in rivers, reservoir-infilling rates, and other historical records (e.g., Minear and Kondolf 2009; Warrick and Farnsworth 2009). Less common, however, is the integration of multiple data sources across a range of spatial and temporal scales to identify specific areas within a watershed with differing rates of sediment production (Ramos-Scharrón and MacDonald 2007) and, subsequently, to quantify their delivery of sediment into downstream receiving waters. However, these steps are critical for identifying and applying effective management actions that depend on the production and delivery of sediment in a watershed (Pelletier 2012).

Our geographic focus for presenting and testing such an approach is the western Transverse Ranges of southern California, where a variety of preexisting studies provide a rich dataset of measured and inferred rates of sediment yield (Scott and Williams 1978; Brownlie and Taylor 1981; Inman and Jenkins 1999; Lavé and Burbank 2004; Romans et al. 2009; Warrick and Mertes 2009; Andrews and Antweiler 2012), where rapid rates of tectonic uplift give rise to a correspondingly large range of (actual or potential) erosion rates, and where a significant human population makes this topic of more-than-abstract interest. This region has already garnered many decades of popular and academic attention because its rapid rates of tectonic activity and sediment delivery in close proximity to a large and growing population (e.g., McPhee 1988). Our contributions to this growing literature are: (1) to describe a rapid, geographic information system (GIS)-based methodology to display the likely distribution of relative sediment yields in this diverse landscape; (2) to quantify those sediment yields under existing land-use conditions; (3) to assess the accuracy of the resulting sediment-yield predictions using independent data sources; and (4) to show how these results can be applied to management concerns in this region.

A Spatially Explicit Representation of Relative Watershed Sediment Yield

Although the conditions and events that detach sediment from hillslopes and subsequently deliver it to river channels are episodic and vary greatly over time (Benda and Dunne 1997; Kirchner et al. 2001; Gabet and Dunne 2003), both geomorphic principles and field observations can readily identify the relative sediment-yield potential of different parts of a landscape.

Study Area

Located in the west part of the tectonically active Transverse Ranges of Ventura County, California, the 674-km^2 Sespe Creek watershed is well-suited for characterizing the processes and natural rates of sediment production and yield (Fig. 1). Sespe Creek is a major tributary to the Santa Clara River, with their confluence adjacent to the town of Fillmore (pop. 15,000). Most of the watershed, however, occupies one of the most pristine and geographically remote areas in all of southern California; it is also one of the few remaining watersheds in the region that lacks any flow regulation or diversion structures, although it has a long-term USGS gaging station near its mouth (USGS 11113000, in continuous operation since 1928). Steep hillslopes mantled with shallow soils (USDA NCSS 2012) characterize most of the physical landscape. Land cover in the Sespe Creek watershed is typical of coastal-draining southern California—upland areas and floodplains, terraces, and valley bottoms in the upper channel network support dense scrub/shrub (chaparral) vegetation; grasslands, and mixed deciduous and evergreen woodlands constitute the remainder of the upland and floodplain land cover. More dense vegetation and larger trees generally concentrate on north-facing slopes, at higher elevations, or adjacent to perennial water sources.

The topographic relief in this mountainous watershed varies from steep upland areas with rugged ridges to a broad, low-gradient valley bottom bordering much of the mainstem channels. Overall, elevations range from approximately 110 to 2290 m above sea level, expressing a landscape of steep relief. Average annual precipitation varies twofold across the watershed, ranging from more than 1,140 mm at Reyes Peak along the Pine Mountains near the headwaters to less than 490 mm near the mouth in the Santa Clara River Valley (1971–2000, from http://prism.oregonstate.edu/). At higher elevations, some winter precipitation is in the form of snow. The five largest floods, based on instantaneous discharge measurements at the USGS gage, were in 1969 (1,700 m^3 s^{-1}), 1978 (2,070 m^3 s^{-1}), 1995 (1,840 m^3 s^{-1}), 1998 (1,770 m^3 s^{-1}), and 2005 (the flood of record, at 2,420 m^3 s^{-1}), which all occurred during years where El Niño–Southern Oscillation (ENSO) conditions prevailed (Cayan et al. 1999; Andrews et al. 2004). The mainstem channel is perennial; mean daily discharge over the full period of record is 3.6 m^3 s^{-1}.

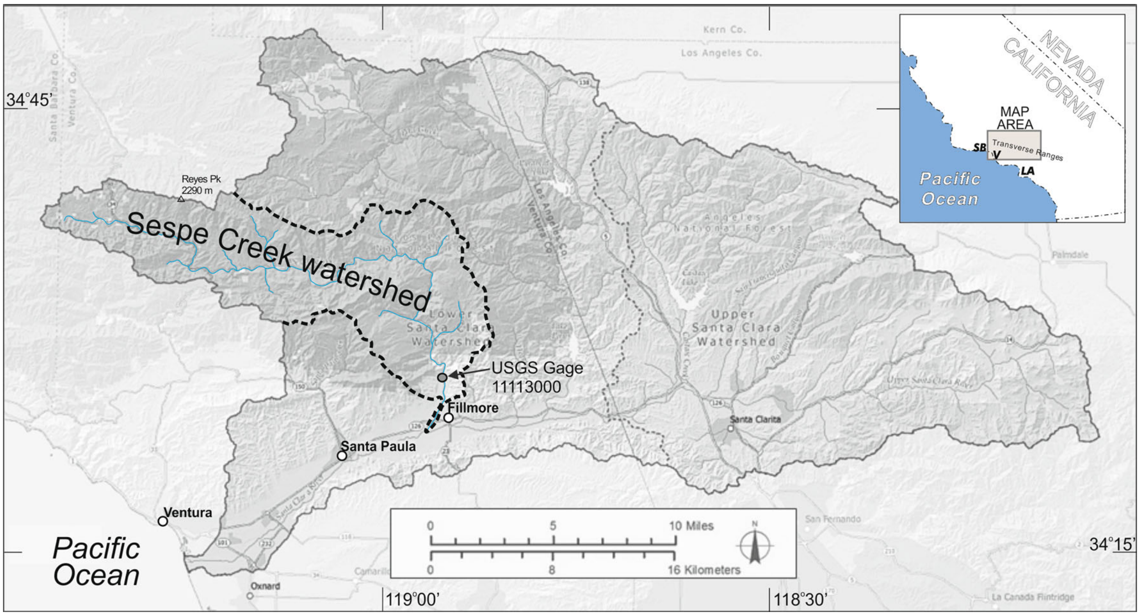

Fig. 1 The 674 km^2 Sespe Creek watershed (*outlined*), contained within the Santa Clara River watershed of southern California. Most of the watershed falls within Los Padres National Forest (*dark shading*); the only major population center in the watershed is adjacent to the town of Fillmore (pop. 15,000), near the mouth of Sespe Creek. USGS gage 11113000 captures 97 % of the watershed drainage area. Cities indicated on *inset map*: *LA* Los Angeles, *V* Ventura, *SB* Santa Barbara

The regional tectonic activity of California over the last 6 million years has created this particular topographic and geologic setting. The San Andreas Fault is deflected from its straight trend here, compressing the north-migrating rocks of the Pacific plate (which include those of the Sespe Creek watershed). In the area of Sespe Creek, one fault expresses this north–south compression most prominently: the north-dipping San Cayetano thrust fault, which cuts west-to-east near the outlet of the watershed. Tertiary volcanic rocks and interbedded marine mudstones, siltstones, sandstones, and conglomerates of the upper block, which includes nearly the entire watershed, have been steeply tilted and uplifted over younger unconsolidated Pliocene and Quaternary sediments (Rockwell 1988; Marshall et al. 2008).

Determinants of Erosion, Production, and Delivery Rates

Determinants of erosion rates, and thus of sediment-production rates, have been cataloged by many decades of prior study. Commonly recognized attributes include the material being eroded (i.e., lithology), a measure of topographic gradient (hillslopes, basin slope), climate (mean annual temperature, mean annual precipitation, climate zone, latitude), land cover (vegetation, constructed cover and imperviousness), and episodic disturbance (e.g., fire, large storms). The actual delivery of sediment to the channel network is further complicated by drainage density, hillside–channel coupling, lag times imposed by the size of the drainage basin, and land use.

Individual studies have tended to focus on a subset of these factors, reflecting both their relative importance and their range of variability within a circumscribed region. Montgomery (1999) suggested that four fundamental factors—regional climate, geology, vegetation, and topography—determine the geomorphic processes over a given landscape. Reid and Dunne (1996) noted that every study area requires simplification and stratification, recommending only topography and geology as the primary determinants with land cover as a “treatment” variable within each topography–geology class. Hicks et al. (1996) identified rock type and rainfall as the major determinants of unit-area sediment yields across New Zealand, but their study sites spanned a 30-fold variability in annual rainfall totals. For any given annual rainfall, they showed 100- to 1,000-fold differences in yields due to lithologic differences, with hillslope gradient providing the only other systematic (but secondary) influence. Walling and Webb’s (1983) review of reported sediment transport trends relative to precipitation found “no simple relationship” between climate and sediment yield. Portenga and Bierman’s (2011) worldwide compilation of ^{10}Be-derived erosion rates for drainage basins found the strongest dependence of erosion rates on basin slope and relief, global climate zone (e.g., “arid” vs. “polar”), and seismicity (“active” vs. “inactive”). Erosion rates in their global data set showed no relationship to either mean annual precipitation or basin area.

Deterministic methods, of which the "Universal Soil Loss Equation" and its various offshoots are the most common, offer an alternative approach. Qualitatively, the USLE identifies precipitation, soil erodibility, topography (in the form of an integration of hillslope gradient and length), and land cover as key determinants. Its approach to quantification, however, depends on both an implicit assumption of erosion processes (i.e., rainsplash, sheetwash, and rilling; Dunne and Leopold 1978) and an underlying calibration data set that is ill-suited to conditions across steep, semi-arid southern California watersheds (e.g., Risse et al. 1993; Kinnell 2005).

In studies localized to the climatological and seismological setting of southern California, prior studies have recognized particularly important determinants of spatially variable erosion rates. Spotila et al. (2002) and Warrick and Mertes (2009) both emphasized the dependency on lithology in the Transverse Ranges, highlighting critical differences between: (1) weakly consolidated Quaternary and Late Tertiary-age marine sediments, and (2) much more competent older sedimentary and crystalline rocks. Gabet and Dunne (2002) found statistically significant differences in shallow landslide frequencies and volumes depending on vegetation cover (sage vs. grassland); Pinter and Vestal (2005) also identified vegetation cover as the primary determinant of landsliding during a single winter of heavy rainfall, with slope angle, slope aspect, slope curvature, bedrock lithology and elevation as secondary factors. In general, a consensus emerges from watershed-scale studies from within this region that geology, topography, and land cover are the primary determinants of the nature and rates of watershed processes, a list that is echoed by other work world-wide, particularly when restricted to a particular geographic (and climatologic) region. Thus, these three factors are carried forward into the current effort.

Methods for Qualitatively Assessing Sediment Production

Each of the three factors used in assessing sediment production and yield (lithology, hillslope gradient, and land cover) was stratified into a limited number of categories, using natural groupings intrinsic to the data. Data sources for each were compiled in a GIS environment over the entire watershed at a resolution determined by the coarsest dataset. This approach for identifying and categorizing those attributes judged to provide a consistent control on sediment production potential is analogous to the long-established concept of "hydrologic response units" (England and Holtan 1969; Beighley et al. 2005). The guiding principle is to define areas that share those key landscape attributes that apply a consistent control on erosion processes and rates, and thus also share similar potential for sediment production. As such, they are a functional application of Montgomery's (1999) concept of "process domains."

Lithologic categories were based on the 1:24,000-scale geologic maps of Dibblee (1985a, b, 1987, 1990a, b, 1996a, b) and grouped into categories of predominantly fine ("shale") and coarse ("sandstone," but also including granite/gneiss), reflecting their low and high likelihood, respectively, of producing the cobbles and sand grains that constitute the bedload sediment in the tributaries and mainstem of Sespe Creek. They also correspond well, although not perfectly, to Warrick and Mertes's (2009) groupings for relatively "weak" and "competent" rocks. Qualitatively, the younger (Miocene and Pliocene) shaley rocks displayed greater erosivity than the older shales (e.g., the Eocene Cozy Dell Formation), particularly on very steep slopes, but this distinction was not made across the watershed because the younger shales occupy only a few percent of the watershed as a whole, and this lithologic category is overall much more erosive than the coarse sandstones and crystalline rocks.

Hillslope gradients were generated directly from the digital elevation model, which in turn was based on a USGS 10-m DEM. Steeper gradients are likely to yield more sediment, but we find no justification for assigning a universal set of threshold values. Gradient categories related to sediment production potential are most defensibly made based on natural breaks in the aggregate distribution of slopes, which likely reflects breaks in landform units and thus potentially differentiates processes (and process rates) that are common to each. In the steep terrain of Sespe Creek (where 84 % of the hillslope values are in excess of 20 %) the continuous range of hillslope gradients was categorized into three groups: 0–20 %, 20–60 %, and steeper than 60 %. A finer discrimination of the flatter slopes (for example, 0–10 %, 10–20 %, > 20 %) may be more appropriate in lowland landscapes; for this application, however, we saw little need for more sophisticated classification techniques (e.g., Iwahashi and Pike 2007).

Land cover was based on a classified 2001 Landsat image at 30-m resolution, previously developed for the entire Santa Clara River watershed (of which Sespe Creek is a major tributary). Five grouped categories were identified based on their relative sediment-production potential, as supported by prior literature (and later confirmed by field observations): (1) forest; (2) scrub; and (3) agriculture and/or grassland and bare soil; (4) developed land; and (5) miscellaneous (a minor category that included water of the river channel itself, where wide enough to register at this scale).

The categories defined for each of these three attributes (lithology, gradient, and land cover) overlap into 30 unique "geomorphic landscape units" (GLUs), each reflecting a combination of the factors judged to be the major determinants of hillslope sediment production and, ultimately, sediment yield from the watershed as a whole. Once mapped, a relative magnitude of sediment production on hillslopes can be assigned to every GLU expressed in the watershed, based on observed indications of erosion and mass-wasting processes, and the proportion of the ground surface that is actively involved in sediment-delivery processes. The coarsest data sets are those for the landcover (raster-based, 30-m pixels), suggesting a final resolution of map data equivalent to a scale between 1:50,000 and 1:100,000.

Results of the Qualitative Assessment

Almost all (28) of the 30 possible GLUs were represented in the watershed, but nearly two-thirds of the watershed area falls into just three: "Sandstone–20–60 %–Scrub" (27.5 % of the watershed area), "Shale–20–60 %–Scrub" (18.6 %), and "Sandstone–>60 %–Scrub" (15.9 %). Only 12 of the possible combinations cover more than 1 % of the total watershed area (Table 1), and in total they account for nearly 97 % of the watershed area. Such spatial dominance of a few of the potential GLU categories is, in our experience, reasonably common and has the effect of making the procedure of field calibration far more feasible than might otherwise appear from a naïve tally of all possible GLUs.

From field observations, relative differences in erosion processes between many of the different GLUs are dramatic and lend confidence to a coarse, threefold division of relative rates (i.e., "High," "Medium," and "Low," henceforth abbreviated H, M, and L) (Fig. 2): in general, "L" areas were uniformly well-vegetated with little to no bare soil, "M" areas were generally stable but with evidence of localized overland flow, and "H" areas displayed extensive erosion and mass wasting, and abundant bare areas. Our observations qualitatively aligned with those of Pelletier (2012, p. 3), who noted "A large proportion of the sediment supplied by many drainage basins is sourced from only a small proportion of the basin where vegetation cover is lower than average, slopes are steeper than average, and conditions otherwise favor high sediment yields." The GIS display of the final GLU categories thus constitutes a predictive map of the relative production of sediment from every part of the watershed (Fig. 3).

This prediction, however, is based only on local attributes at each location in the watershed, and so it does not account for any routing or storage of sediment on the hillslopes or within the channel network. This simplifying assumption appears to be warranted on Sespe Creek and other such high-relief watersheds, because storage capacity in the system is observed to be low and so sediment delivery to the channel is a large fraction of the magnitude of hillslope erosion (Fig. 4). However, watershed data are available to evaluate, at least indirectly, the consequence of this assumption and are discussed below.

Table 1 Geomorphic landscape units (GLUs) in the watershed as a percent of total watershed area ("–" = <1 % of total area)

Geomorphic landscape units	% of watershed	Relative sediment production
Sandstone–0–20 %–Forest	1.5	Low
Sandstone–20–60 %–Forest	3.9	Low
Sandstone–>60 %–Forest	2.8	Low
Sandstone–0–20 %–Scrub	7.9	Medium
Sandstone–20–60 %–Scrub	27.5	Medium
Sandstone–>60 %–Scrub	15.9	Medium
Sandstone–0–20 %–Ag/grass/bare	1.0	Medium
Sandstone–20–60 %–Ag/grass/bare	–	Medium
Sandstone–>60 %–Ag/grass/bare	–	High
Sandstone–0–20 %–Developed	–	Medium
Sandstone–20–60 %–Developed	–	Medium
Sandstone–>60 %–Developed	–	Medium
Sandstone–0–20 %–Misc.	–	Medium
Sandstone–20–60 %–Misc.	–	Medium
Sandstone–>60 %–Misc.	–	Medium
Shale–0–20 %–Forest	–	Low
Shale–20–60 %–Forest	2.1	Low
Shale–>60 %–Forest	1.9	Low
Shale–0–20 %–Scrub	2.8	Medium
Shale–20–60 %–Scrub	18.6	Medium
Shale–>60 %–Scrub	11.0	Medium
Shale–0–20 %–Ag/grass/bare	–	Medium
Shale–20–60 %–Ag/grass/bare	–	High
Shale–>60 %–Ag/grass/bare	–	High
Shale–0–20 %–Developed	–	Medium
Shale–20–60 %–Developed	–	Medium
Shale–>60 %–Developed	–	Medium
Shale–0–20 %–Misc.	–	Medium
Shale–20–60 %–Misc.	–	Medium
Shale–>60 %–Misc.	–	Medium

Relative sediment production category as noted for each, based on qualitative field observations (Fig. 2); relative sediment production of GLUs unrepresented or of very limited extent was inferred from related values

Quantifying Sediment-Production Rates in Sespe Creek Watershed

The fundamental utility of GLUs lies in their spatially explicit prediction of differences in sub-watershed-scale

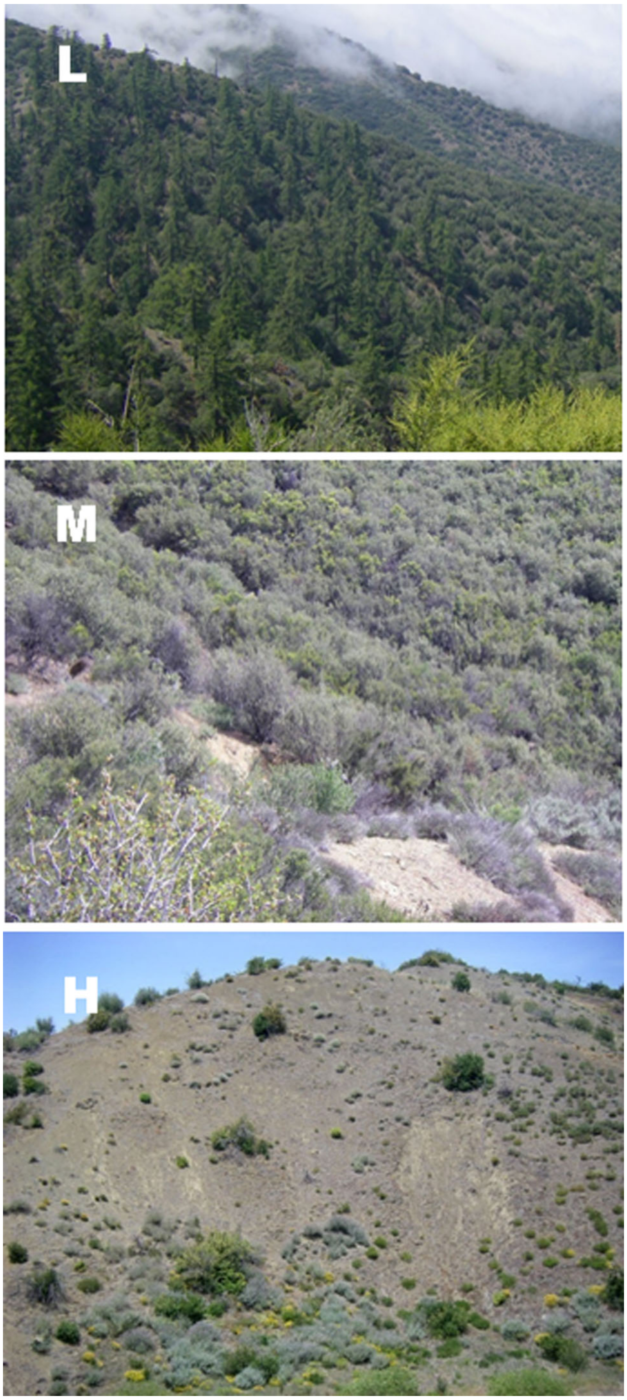

Fig. 2 Examples of different geomorphic landscape units (GLUs) and their relative levels of sediment production. *Top* Sandstone–20–60 %–Forest; *middle* Shale–20–60 %–Scrub; *bottom* Shale–>60 %–Ag/bare

rates of sediment production. Quantification of these rates is not required for many applications in environmental management, but if relevant data are available then additional benefits can be achieved as well. Such data include the sediment-infilling rates of reservoirs and smaller basins (together with a variety of other field techniques and regional compilations), which have long been used to develop quantitative estimates of watershed sediment yield (see the extensive discussion and source materials in Reid and Dunne 1996). Fortuitously, debris basins are widespread across the southern California landscape, providing a rich data source for quantifying yields here. In the general vicinity of Sespe Creek, lengthy records spanning many decades have been maintained by the Ventura County Watershed Protection District (VCWPD 2005) on the volumes of sediment excavated from multiple debris basins in their jurisdiction.

Rates of Sediment Yield from Nearby Debris Basins

From the population of all debris basins within the Santa Clara River watershed (of which Sespe Creek is a part), the five closest to the Sespe Creek watershed were identified (including one, Jepson Wash, within the watershed itself) (Table 2; Fig. 5); all collect their runoff from the same suite of Tertiary to Quaternary sedimentary rocks found in the watershed. Only those years of accumulation following the first recorded excavation of the basin were tallied (so the beginning and ending times at all sites were under equivalent, empty conditions). Although capture ratios of debris basins are never determined directly and surely none achieve 100 % trapping efficiency, the location of the facilities—low in their respective catchments within relatively low-gradient topography—suggests that the raw data provide a crude, if somewhat conservative, estimate of the sediment volumes delivered to them.

These calculated sediment yields form the basis of calibrating unit-area sediment yields for the three categories of GLUs, as described below. Their range is very similar to that reported by Lavé and Burbank (2004), who used a more extensive set of sediment-removal records from approximately 115 debris basins located ten to several tens of kilometers east in the southern foothills of the San Gabriel Mountains, draining watersheds with records ranging from 9 to 68 years long of similar topography, lithology, and land cover. There, they found rates of 200 to 14,700 t km^{-2} $year^{-1}$ of sediment production from the watersheds that feed them, with the lowest values draining resistant crystalline bedrock that is of only limited extent in Sespe Creek (and not at all in the contributing area of the five debris basins of Table 2).

Quantifying GLU Categories with the Debris-Basin Data

The long-term debris-basin data from the region provide an opportunity to quantify the relative contribution of individual GLUs previously categorized as “High,” “Medium,”

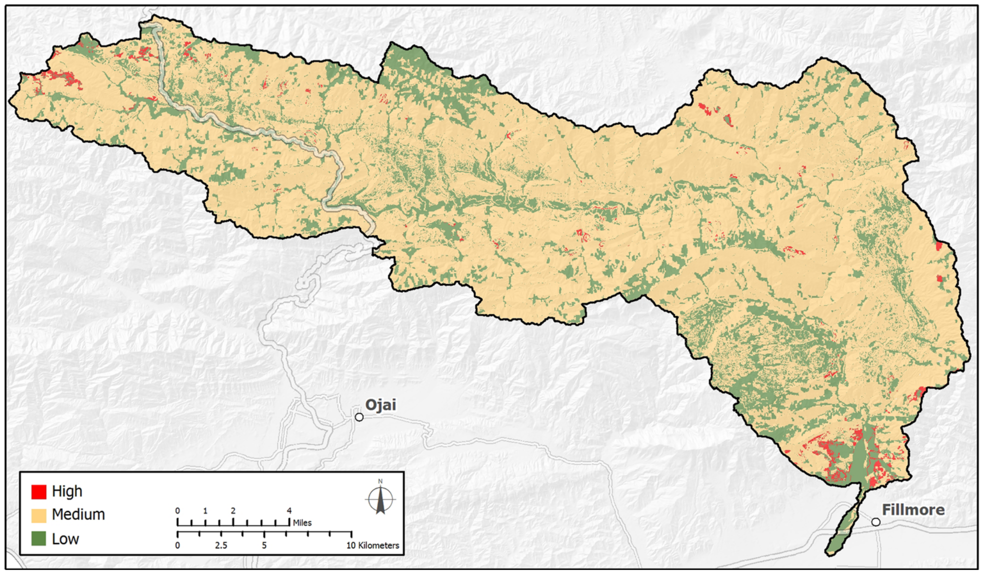

Fig. 3 Predicted sediment production in the Sespe Creek watershed upstream of USGS gage 11113000. The majority of the watershed is "Medium" (*mustard color*); less than 1 % is "High" (*red*; mainly flanking the lower valley and in the extreme western headwaters), with scattered areas of "Low" (*light gray*) particularly on well-vegetated north-facing slopes (Color figure online)

Fig. 4 Example of the close coupling of hillslopes and channel, and the lack of significant volumes of stored sediment, which lends support to the omission of this element of sediment budgeting in the GLU analysis

and "Low." Within each of the tributary areas to the five debris basins, GLUs were defined and the individual pixels assigned to H, M, and L sediment-yield categories using the same procedure as for the Sespe Creek watershed as a whole. All five basins were visited in the field, to insure that the contributing watersheds were generally representative of the Sespe Creek-area landscape in terms of sharing the same sediment-production determinants and there being no substantive differences in land-use activities or infrastructure (besides the debris basin itself).

To determine specific numeric values of sediment delivery for the relative GLU categories of H, M, and L, we began with values suggested by both prior work (particularly maximum reported debris-basin averages in VCWPD (2005) and Lavé and Burbank (2004) for "H," whole-watershed averages from Warrick and Mertes (2009) for "M," and minimum regional values reported by Lavé and Burbank (2004) for "L"). We then considered multiple combinations of sediment-delivery factors, identifying the set of values that minimized the sum of the ratios of predicted-to-measured values for the five debris basins (Fig. 6). The optimal set is H = 25,000, M = 3000, and L = 200 t km^{-2} $year^{-1}$, although there is clearly uncertainty with any given choice of parameters.

Applying these factors to the Sespe Creek watershed as a whole predicts an average annual total sediment yield of 1,670,000 t $year^{-1}$ (2,600 t km^{-2} $year^{-1}$). Although by convention these rates are all expressed on a "per year" basis, both geomorphic principles and common sense acknowledge that actual sediment production and delivery are highly episodic, with many years of relatively little production punctuated by erratic pulses of very high delivery associated with large storms (Benda and Dunne 1997; Inman and Jenkins 1999; Gabet and Dunne 2003). Historical records from the Sespe Creek gage suggest that year-to-year variability may be of the same order, or more, as the predicted "annual" values themselves (see also Farnsworth and Milliman 2003; Andrews and Antweiler 2012).

Although GLUs are classified at a scale determined by 30-m pixels, the results are not useable at so fine a scale. This is because the GLU sediment-yield values were calibrated using measurements from debris basins whose catchment areas aggregate many individual GLUs into watersheds that range from 0.6 to 22 km^2 (i.e., ca. 1,000 to 25,000 individual pixels), or from whole-watershed rates of sediment production and sediment yield with even larger total drainage areas. We have used these aggregated data to

Table 2 Debris basin data from Ventura County used to quantify rates of sediment delivery in the Sespe Creek watershed

Name	Contrib. area (km^2, from GIS)	Annual average sediment yield (yd^3 $year^{-1}$)[a]	Sediment yield per unit area (t km^{-2} $year^{-1}$)	Equivalent watershed denudation rate (mm $year^{-1}$)[b]	Years evaluated[a]	Location relative to Sespe watershed
Real Wash	0.6	7,423	26,670	7.3	1969–2005	12 km east
Warring Canyon	2.8	12,039	6,960	2.5	1969–1998	12.4 km east
Jepson Wash	3.5	9,174	4,030	1.5	1969–2005	Southwest corner
Fagan Canyon	7.5	12,500	3,670	1.0	1994–2005	12 km south
Adams Barranca	21.8	27,362	1,110	0.7	1998–2005	13 km south

[a] *Source* VCWPD (2005), in units as originally reported

[b] Bulk density assumed to 1.9 t m^{-3} based on estimated bulk densities reported for nearby debris basins in Los Angeles County (Lavé and Burbank 2004)

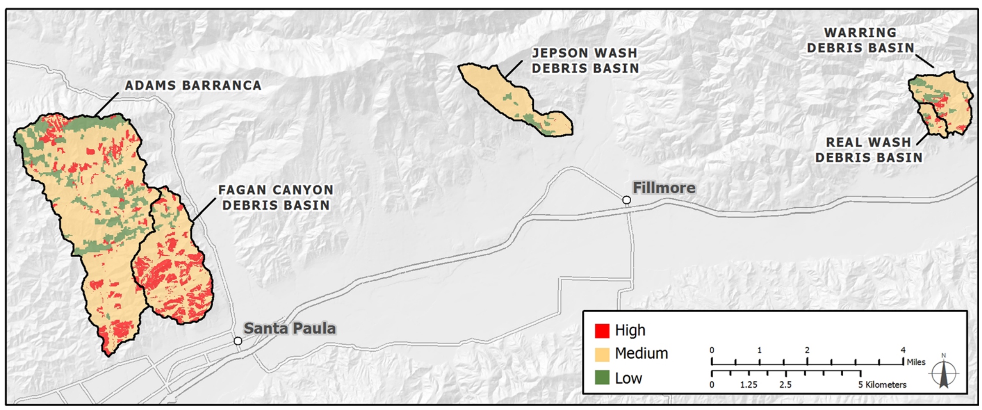

Fig. 5 Five nearby watersheds draining into debris basins with records of sediment removal, used to calibrate sediment-yield values for "High," "Medium," and "Low" geomorphic landscape units (GLUs). *Color scheme* as for Fig. 3 (Color figure online)

calibrate our unit-area values for reasons both pragmatic and fundamental. Pragmatically, individual plot-scale measurements are simply not available for most of the potential GLU types here (as in most management applications). More fundamentally, plot-scale measurements (even if available) do not incorporate downslope transport and storage that affects how much sediment is actually delivered to the channel network. By applying the GLU analysis at the same general scale as the measurements used to quantify their associated sediment-yield rates, we seek to avoid the long-recognized scale dependency of sediment delivery (Walling and Webb 1983) and expect that our results will incorporate the influence of those additional processes, even if we are unable to precisely quantify their effects.

Accuracy of Predicted Rates of Sediment Yield

Our GLU approach provides spatially explicit rates of sediment production suitable for decadal-scale application to those environmental management issues that depend on rates of sediment production, transport, and delivery. GLUs yield rates were calibrated; but because we lack plot-level monitoring or a wide network of small watershed sediment gages, true "validation" of such an approach is impossible (and generally infeasible for most management applications, regardless). It is thus imperative that the general accuracy of the approach is assessed by whatever available independent data exist. To that end, we have sought a multi-proxy approach using independent data sources across a range of spatial and temporal scales.

Rates of Sediment Yield Inferred from Geologic Evidence

Watershed topography reflects the interplay between uplift (if any) due to tectonic processes and the sculpting and wearing away of slopes by erosion. The linkages between uplift, slope steepness, and erosion imply that slopes should tend to contribute sediment in proportion to their uplift rates over the long-term (Burbank et al. 1996; Spotila et al.

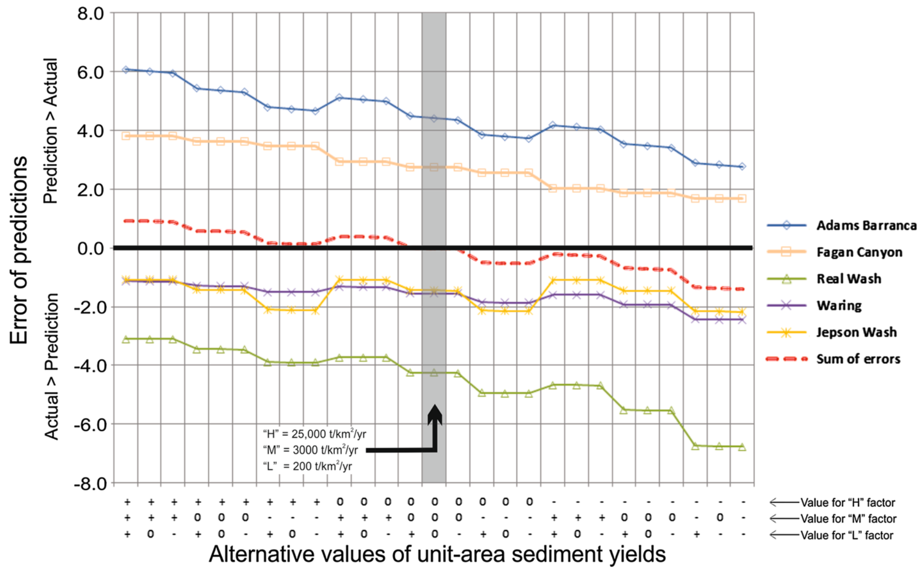

Fig. 6 Evaluation of how well alternative values for unit-area sediment yields predict actual debris basin sediment yields. "Actual" values were calculated from measured sediment-removal volumes from five basins (VCWPD 2005; Table 2), and they are expressed as ratios of the "predictions" calculated from presumed values for H, M, and L GLU types as mapped on Fig. 4. Also graphed is the arithmetic "sum of errors" of the individual errors from the 5 debris basins (*thick dashed line*), with the assumption that a zero net error provides the best estimate. Symbols along the *x*-axis reflect the various combination of values used for H (*top symbol*), M (*middle symbol*), and L (*bottom symbol*). "0 0 0," which has the best aggregate performance with a near-zero sum of errors (*gray-shaded band*), represents H = 25,000, M = 3,000, and L = 200 t km^{-2} year^{-1}. Results of the combinations displayed here encompass increases to these values (shown by "+") of 10,000, 1,000, and 100 t km^{-2} year^{-1} for H, M, and L factors, respectively; and reductions by the same amounts (shown by "−"). Thus, for example, the combination symbolized by "+ + −" has assumed values of H = 35,000, M = 4,000, and L = 100 t km^{-2} year^{-1}

2002)—rapid uplift rates therefore usually result in high rates of erosion and sediment yield. Uplift rates, in turn, are directly related to the tectonic setting and deformation history of the landscape.

Long-term average uplift rates from the region's mountain ranges are among the fastest on record for the continental United States, reflecting complex processes at the boundary between two tectonic plates (Blythe et al. 2000; Meigs et al. 2003). Several tens of km east of Sespe Creek in the San Gabriel Mountains, Blythe et al. (2000) looked at the cooling history of mineral grains to find likely uplift rates averaging as high as about 1 mm year^{-1} in the eastern San Gabriel Mountains, with less well-determined but significantly lower rates in the western San Gabriel Mountains. West of Sespe Creek, uplift rates for the Santa Ynez Mountains range from 0.75 to >5 mm year^{-1} (Metcalf 1994; Trecker et al. 1998; Duvall et al. 2004). A summary of uplift rates for the coastline within the Transverse Ranges region reports an even broader range of 0.05–9 mm year^{-1} (Orme 1998).

Movement across the major faults in and around the Sespe Creek watershed drive uplift of the landscape; reported rates vary from place to place but are everywhere rapid (in geologic terms). Immediately southwest in the adjacent Santa Paula Creek watershed (immediately north of the town of Santa Paula; Fig. 1), an uplifted fluvial terrace now lies 13 m above the level of modern fluvial deposition with an inferred age of 15,000–20,000 years (Rockwell 1988), giving an uplift rate between 0.65 and 0.87 mm year^{-1}. One kilometer east of this locale, Rockwell (1988) also identified a younger alluvial fan (estimated age 8,000–12,000 year) with about 9 m of vertical offset, giving a rate of 0.6–1.2 mm year^{-1}. In this same area but using older landforms, he also inferred an uplift rate of as much as 1.6 ± 0.2 mm year^{-1} over the past 80,000–100,000 years. Rockwell (1988) also inferred that uplift rates increase to the east along the 40-km-trace of the San Cayetano Fault; just east of Fillmore at the eastern edge of the Sespe Creek watershed, he argued that this fault displayed at least 7.5 km of motion in the last 1 Ma on the basis of stratigraphic offset. With a reconstructed dip of 30°–40° on the main fault plane, this amount of movement along the sloping surface translates into an equivalent vertical (i.e., uplift) rate of ≥4 mm year^{-1}. Çemen (1989) also evaluated uplift rates on the San Cayetano Fault east of Sespe Creek between the towns of Fillmore and Piru. His results closely match those of Rockwell (1988), with an estimated 7.3 km of fault offset over the ∼1 Ma of the fault's existence.

Just west of the Sespe Creek watershed, Huftile and Yeats (1995) evaluated overall shortening across the Transverse Ranges. Here they concluded that the magnitude of shortening across the region was most likely about

Table 3 Summary of published uplift rates in the Transverse Ranges region, expressed in terms of uplift and equivalent production of sediment under the assumption of a steady-state landscape

Location	Rate expressed as landscape denudation rate (mm year^{-1})			Rate expressed as sediment production (t km^{-2} year^{-1})[a]			References
	Low	High	Average	Low	High	Average	
San Cayetano Fault	1.1	9	–	3,000	23,000	–	Rockwell (1988)
Santa Ynez Mts. (immediately W of Sespe)	0.7	>5.0	–	2,000	13,000	–	Metcalf (1994), Trecker et al. (1998), Duvall et al. (2004)
Transverse Ranges (all)	0.05	9	–	130	23,000	–	Orme (1998)
Holser Fault (E extension of San Cayetano Fault)	>0	0.4	–	>0	1040	–	Peterson et al. (1996)
Santa Susana Fault (~20 km SE of Sespe)	>2	>8	–	>5,200	>21,000	–	Peterson and Wesnousky (1994), Wills et al. (2008)
San Gabriel Mts. (~30 km E of Sespe)	<0.1	1.0	–	<260	2,600	–	Blythe et al. (2000)
San Gabriel Granite	0.05	0.46	0.29	130	1200	750	Heimsath (1998, Appendix 2)

[a] Uplift rates are converted to sediment production units under the assumption that rates of mountain uplift are fully balanced by rates of bedrock erosion using a presumed bedrock density = 2.65 t m^{-3}. "Average" value shown only where reported by the original source

5 km in the last 500,000 years, of which about one-third was taken up across the San Cayetano Fault. This yields a horizontal shortening rate across the fault of 3–4 mm year^{-1}; because their reconstructed fault angle is about 45° here, the resulting uplift rate would be of equivalent magnitude.

In total, published rates of crustal uplift in and surrounding the Sespe Creek watershed range from about 0.7 mm year^{-1} to more than ten times this value (Table 3). Over the last 1 million years, estimates of rates range between 3 and 6 mm year^{-1}. Uplift is certainly continuing into modern time (Donnellan et al. 1993; Marshall et al. 2008; Argus et al. 1999), and the magnitude of vertical change within the watershed most likely lies within the range of 2–4 m per thousand years. "Uplift rates," however, do not directly correlate with rates of erosion or sediment yield, and the geomorphic evidence from the Sespe Creek watershed indicates that these uplift rates are at least comparable to (and likely greater than) hillslope erosion rates here. Evidence of higher uplift rates is primarily in the form of preserved, uplifted landforms, because faster degradation rates would presumably have consumed these features (Burbank et al. 1996). For example, multiple stream terraces having a bedrock core on the upthrown (northern) block of the San Cayetano Fault are prominent, both adjacent to the fault trace itself near Fillmore and throughout the upper watershed (Gutowski 1978). Thus, the magnitude of steady-state sediment yield implied by these uplift rates, about 5,000–10,000 t km^{-2} year^{-1}, provides an upper limit on credible rates of sediment yield from the watershed as a whole.

Rates of Sediment Yield from Measured Sediment Discharge

Long-term watershed sediment yield rates can also be derived from direct in-channel sediment measurements. We compiled the sediment load data from the USGS gage near the mouth of Sespe Creek (USGS gage 11113000) to develop a sediment rating curve and an average annual total sediment yield estimate. Available suspended sediment load data from 1966 to 1992 were first compiled and related to the instantaneous discharge for individual suspended sediment loading measurements (Fig. 7a). Total sediment load was then calculated by increasing suspended load measurements by 10 % to account for bedload contribution, which was based on findings from earlier work in the region (e.g., Williams 1979; Andrews and Antweiler 2012) and from comparing the limited available bedload measurements to the suspended sediment load data (Fig. 7b). The newly developed total sediment load data were then regressed against instantaneous discharge, which showed an inflection in the sediment loading-discharge relationship at a discharge of 10 m^3 s^{-1} that motivated separate regression equations (i.e., total sediment rating curves) above and below this value (Fig. 7c). To assess the uncertainty associated with an average annual total sediment load estimate, the 95 % prediction interval for both total sediment rating curves was determined as a function of local standard error for the data associated with each regression equation. The total sediment rating curves were then combined with the daily mean flow to determine a time series of daily total sediment loading. Finally, these loading values were

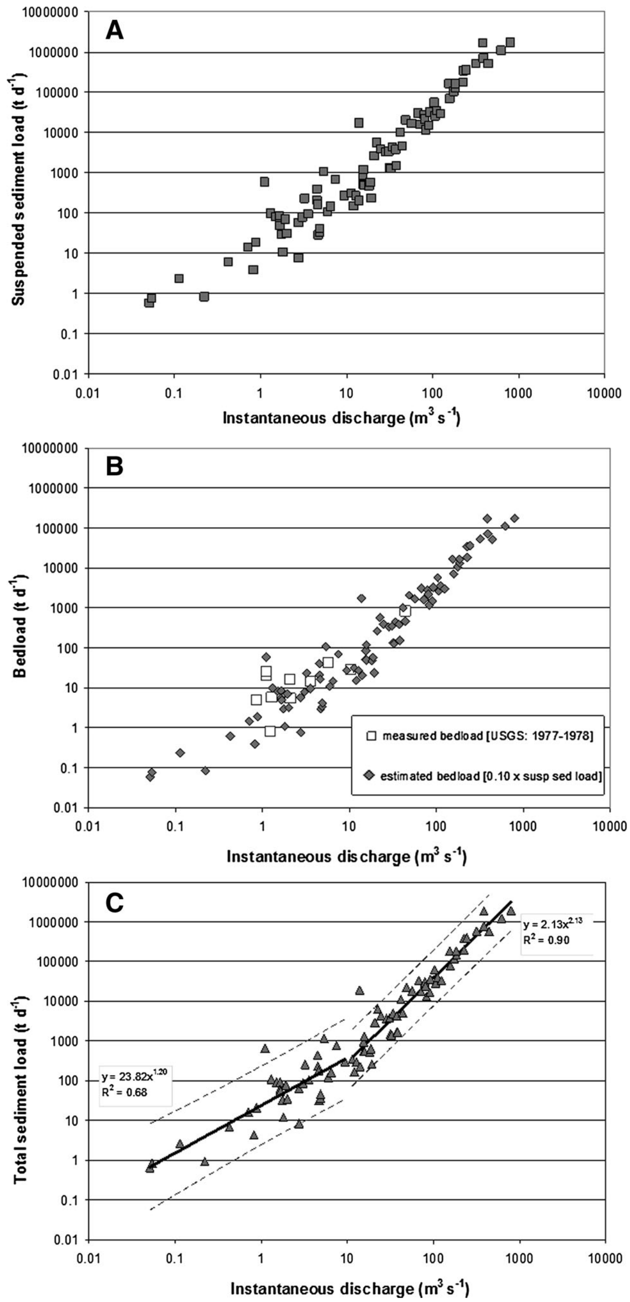

Fig. 7 Sediment data for Sespe Creek (USGS gage 11113000). **a** Measured suspended sediment load from 1966 to 1992; **b** Measured bedload from 1977 to 1978, and calculated bedload as a function of measured suspended load; **c** Calculated total sediment load with power regressions (*solid lines*), regression equations, and 95 % prediction intervals (*dashed lines*) for the data above and below 10 m^3 s^{-1}

increased by a gage-specific correction factor that accounts for using daily mean flow in a hydrologically "flashy" setting (per the analysis by Warrick and Mertes 2009) and summed to determine annual total sediment yield.

Over the 81-year discharge record (1928–2009), this analysis predicts an average annual total sediment yield at the Sespe Creek gage of about 1,700 t km^{-2} year^{-1}, with 95 % confidence that the true average annual yield is within a factor of five of this value. By comparison, Warrick and Mertes (2009) used the same sediment data over a shorter period from 1966–1999 (but one that more closely overlaps with our debris-basin data of Table 2) to calculate an average annual suspended sediment yield of 2,300 t km^{-2} year^{-1} ($\sim$2,500 t km^{-2} year^{-1} if an estimated bedload contribution equal to 10 % of the suspended load is included). Since Warrick and Mertes' (2009) period was only 40 % of the full record but included four of the five largest annual peak discharges in the entire record, our longer record is likely a more reliable estimate of long-term average sediment yield from the watershed, but the span of calculated values also provides a reminder of the range of uncertainty in any such results. The gage data thus support an annual total sediment yield of about 2×10^3 t km^{-2} year^{-1} within the Sespe Creek watershed (which corresponds to a watershed lowering rate of about 0.8 mm year^{-1}).

Comparison of Approaches

The GLU-based estimate of total watershed sediment yield, derived strictly from the aggregation of classified landscape regions with unit-area sediment yield values assigned and calibrated from local debris-basin data, predicts a total annual rate of 2,600 t km^{-2} year^{-1} (equivalent to a watershed-averaged landscape lowering rate of about 1 mm year^{-1}). This rate is less than half of the current best estimate of landscape uplift rates. However, the modern landscape displays widespread preservation of relict landforms, particularly bedrock-cored river terraces that stand above the level of the modern fluvial system, which demonstrate a past and ongoing imbalance between regional uplift and watershed erosion that offers a crude but critical constraint on any credible prediction of sediment yields. More precise evaluation of the accuracy of the GLU approach is provided by 26 years of measured suspended sediment data, which has been extrapolated to generate yields that align broadly or quite precisely (depending on the chosen period of record) with the GLU-based estimate. This correspondence is achieved even though the gage-based data includes the effects of sediment storage and delivery losses between hillslopes and the basin outlet at the full watershed scale, processes not explicitly included in the GLU approach.

We therefore affirm a good overall level of agreement across the various estimates of sediment yield that lend confidence to the GLU-based "representative area" approach. Although measured data (such as from the Sespe Creek gage) might be considered a superior record and thus obviate the need for the more computationally intensive, assumption-bound approach that we present here, the benefits of using GLUs to characterize sediment yield across a watershed are substantial: (1) they provide a spatially explicit identification of primary sediment sources; (2) they provide a rapid method to assess the local or watershed-wide consequences of land-cover changes; and (3) they can be applied, albeit with less confidence, where confirming data are unavailable (although some basis to calibrate the unit-area yield rates must still exist). Some examples of these capabilities are provided in the following section.

Applications of the Approach

Sediment-Related Impacts of Wildfire

Within chaparral-dominated watersheds, such as in the western Transverse Ranges, wildfire can cause a shift in the relative importance of the few dominant sediment-production mechanisms that occur in this type of environment, chiefly through removal of vegetative cover and alteration to soil conditions (Wells 1981, 1987). During and directly following wildfires in chaparral watersheds, but before the first post-fire rainfall occurs, sediment production is dominated by a pulse of dry ravel as granular sediment stored behind organic barriers (e.g., stems, downed branches, organic litter) is liberated when these barriers are incinerated (Shakesby and Doerr 2006). Surface erosion of the now more friable, less cohesive hillslope materials is thereby enhanced several-fold during the initial post-fire rainfall event(s) through increased direct rainsplash impact and reduced surface infiltration that, together, intensify overland flow (Doerr et al. 2000; Moody and Smith 2005; Cannon et al. 2008; Wohlgemuth and Hubbert 2008).

Any attempt to predict quantitative these increases in sediment production as a result of fire, however, is confounded by the complexity of hillslope and vegetation changes as a result of fire, the stochastic interplay of burn areas and intense rainstorms in the several years immediately following of a fire, and the variable range of reported field-measured factors (Shakesby and Doerr 2006; Wohlgemuth and Hubbert 2008). We nonetheless suggest that our analysis of GLUs in burned areas, in combination with regionally published results, can provide order-of-magnitude constraints on the locations and likely range of consequences to sediment yield in the watershed.

Prior Analysis Using the US Forest Service's "BAER" Method

In September 2006, the Day Fire swept through the Los Padres National Forest, including large portions of the Sespe Creek watershed. The fire, the seventh largest on record in California, burned approximately 655 km^2 (USFS 2006) including 224 km^2 (about one-third) of the Sespe Creek watershed. The Day Fire raised concerns over fire effects on short-term and long-term sediment delivery dynamics and bed elevation change (i.e., flood-protection capacity) near the town of Fillmore, and it was the primary motivation for the present investigation.

Sediment yield in the Sespe Creek watershed following the Day Fire was first estimated as part of the United States Forest Service Burned Area Emergency Response (BAER) assessment (USFS 2006). The Day Fire BAER assessment used the methodology detailed in Rowe et al. (1949), who used sedimentation records from reservoirs and debris basins in Los Angeles County to determine the relationship between peak flow and sediment delivery for individual unburned debris basins under a wide variety of flow conditions. The resulting relationships were then used in the BAER assessment to predict pre- and post-fire annual sediment yield for Sespe Creek near the mouth at the town of Fillmore. The BAER assessment concluded that a suite of fires that occurred in the Sespe Creek watershed between 2002 and 2006 (including the less extensive Wolf and Piru fires plus the Day Fire) resulted in a net increase in sediment yield of about 5.3×10^6 t from the Sespe Creek watershed, with most of increased sediment coming from the areas burned in the Day Fire (USFS 2006) in the first year post-fire.

Analysis Using Geomorphic Landscape Units

The changes to erosion processes as a result of wildfire are amenable to (admittedly simplified) representation using the GLU approach. We have explored the utility of this framework simply by changing the GIS representation of all vegetated land-cover classes in the "burn area" to that of bare ground, and then reassigning all affected GLUs into their appropriate new category (e.g., Shale–20–60 %–Forest becomes Shale–20–60 %–Ag/grass/bare). This in turn changes the sediment-production category of several of the original GLUs (Table 4), reflecting the implicit assumption that the dominant erosion processes have similarly changed in the manner implied by the altered GLU categories. In the area of the Day Fire itself, an order-of-magnitude increase is predicted by the GLUs (reflecting the change from predominantly "Medium" to "High"-rated pixels, with associated unit-area factors of 3,000 and 25,000 t km^{-2} $year^{-1}$). These changes within the burned areas are predicted to result in about 6×10^6 t more sediment from the Sespe Creek watershed, relatively close to (and much more rapidly calculated than) the prediction of the BAER assessment (above).

Of course, the timing of subsequent rains determines the actual consequence of a given fire on the sediment loads. After just a single year post-fire, the magnitude of sediment

Table 4 Categories of relative rates of sediment production assigned for the post-fire scenario for the dominant GLUs found in the Sespe Creek watershed

Geomorphic landscape unit	Original sediment-production rating[a]	Fire scenario sediment-production rating
Shale–0–20 %–Forest	Low	Medium
Shale–20–60 %–Forest	Low	High
Shale–>60 %–Forest	Low	High
Sandstone–20–60 %–Forest	Low	High
Sandstone–>60 %–Forest	Low	High
Sandstone–20–60 %–Misc.	Medium	High
Sandstone–>60 %–Misc.	Medium	High
Sandstone–20–60 %–Scrub	Medium	High
Sandstone–>60 %–Scrub	Medium	High
Shale–20–60 %–Developed	Medium	High
Shale–20–60 %–Misc.	Medium	High
Shale–>60 %–Misc.	Medium	High
Shale–20–60 %–Scrub	Medium	High
Shale–>60 %–Scrub	Medium	High

[a] Ratings from Table 1

increase substantially declines as vegetation begins to reestablish; after no more than a few years, rates tend to return to values more typical of the long-term averages (Prosser and Williams 1998; Shakesby and Doerr 2006). The GLU analysis thus carries a cautionary note for any single-year prediction of post-fire erosion, although it can characterize both the magnitude of likely fire-induced sediment increases and the trajectory of recovery as vegetation reestablishes.

Coarse Sediment Delivery

With detailed knowledge of local rock types, it is possible to use the GLU framework to predict preferential production of broad sediment-size categories. In particular, isolating the coarse fraction of the sediment load can be important to a range of management concerns because of the overriding influence of this material on the bedload and morphology of the river, factors of particular importance in evaluating the potential for aggradation of the channel and floodplain with respect to flood protection and channel migration. It can also be critical in determining the structure of fish habitat (e.g., Downs and Booth 2011). In Sespe Creek, areas having sandstone- or granite/gneiss-dominated lithologies were identified from lithologic descriptions and field observation as being the primary contributors of coarse material to the channel, together with modern and older fluvial deposits (which have a high proportion of cobbles and boulders) (for example, Fig. 4).

Table 5 Relative rates of coarse sediment delivery by geomorphic landscape unit

Geomorphic landscape unit	Coarse sediment production rate
Sandstone–0–20 %–Ag/grass/bare	Low
Sandstone–0–20 %–Misc.	Low
Sandstone–0–20 %–Developed	Low
Sandstone–0–20 %–Forest	Low
Sandstone–20–60 %–Forest	Low
Sandstone–>60 %–Forest	Low
Sandstone–0–20 %–Scrub	Low
Sandstone–20–60 %–Misc.	Medium
Sandstone–20–60 %–Developed	Medium
Sandstone–>60 %–Developed	Medium
Sandstone–20–60 %–Scrub	Medium
Sandstone–>60 %–Scrub	High
Sandstone–20–60 %–Ag/grass/bare	High
Sandstone–>60 %–Ag/grass/bare	High
Sandstone–>60 %–Misc.	High

GLUs were thus assigned and mapped into relative levels of coarse sediment production (Table 5; Fig. 8).

Inspection of Fig. 8 emphasizes several features of the predicted sources of coarse sediment. First, sources of coarse sediment are widely distributed across this watershed, and so the channel likely has ready access to coarse sediment throughout its length. Second, about 15 % of the total map area is predicted to be zones of "high" delivery, with field inspection showing that their delivery ratio is typically high because of few impediments to the processes, primarily debris flows originating in steep valley sides and rockfalls directly into the channel, that deliver coarse blocks to the channel network. Unlike the GLU predictions of total load for this watershed, however, there are no measured data to provide numeric values to the relative categories of "High," "Medium," and "Low" for coarse sediment production (or to their spatial integration across the watershed as a whole) so the prediction is only one of relative spatial distribution of coarse sediment rather than of absolute rates.

Potential Application to Other Regions

Experience with this approach in other parts of southern and south-central California (e.g., Booth et al. 2010) suggests that the conceptual framework underpinning this "representative area" approach supports a useful and robust method for systematically identifying areas of a watershed with different relative contributions to the total sediment load of the downstream river. Four elements of

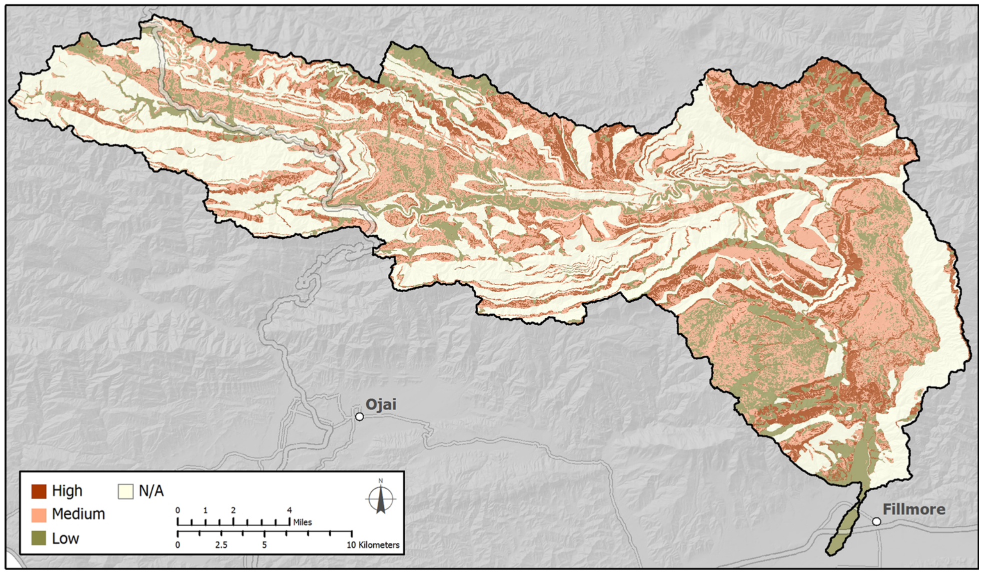

Fig. 8 Predicted coarse sediment production in the Sespe Creek watershed. Of the portion of the watershed underlain by sandstone, areas of relative levels of production are colored *dark brown* ("High"), *pink* ("Medium"), and *green* ("Low"). *Pale yellow* areas are not assumed to produce any coarse sediment by virtue of their mapped lithology (Color figure online)

the approach, however, are likely to require consideration before transferring the technique to other locations.

1. *Range of variability in sediment production* As a fundamentally qualitative assessment of relative sediment-production rates, this approach will be most successful where the absolute range of those rates is large, and thus the importance of nuanced (and potentially subjective) differences between landscape attributes is limited. Regions with only minor differences in lithologic properties or land cover, or with low topographic relief, will likely lack strong spatial differences in sediment production. In such areas, application of the GLU approach would almost certainly be more idiosyncratic, but even if well-executed it might offer only limited insight to managers—other issues, requiring other approaches, should be the focus of environmental assessments there.
2. *Relevant parameters* For the range of applications to date, in watersheds from 100's to 1,700 km^2 within the Transverse Range and Central Coast regions of California, the relevant controlling variables appear to be lithology, gradient, and land cover. However, for larger watersheds or those with substantial topographic relief, factors such as spatial differences in precipitation may have the potential to impose variability as great as the other parameters (e.g., Hicks et al. 1996; Pelletier 2012) and so may require integration into the GLU method. Likewise, sediment-production rates associated with GLU categories may need adjusting if comparing tectonically active to non-active watersheds, or where there is a strong and overriding influence of a point-based human influence (such as watersheds where the sediment supply is disconnected due to a large dam).
3. *Categorical divisions* The accuracy of the approach depends, in large part, on the categorical division of the individual data sets into a manageable number of GLUs. The subdivisions applied here are drawn from geologic and geomorphic literature that affirms distinct sediment-production responses from the different categories of geology, slope, and land use. In each new terrain, however, a robust defense is required for the assignment of lithologic categories and for identifying natural breaks in hillslope gradient. The number of categories chosen for each data layer is a matter for considered judgment: more than about 3–5 categories for each layer will result in a number of potential GLUs well beyond the capacity of a feasible field-verification effort. Even with thoughtful category selection, this overall approach is not amendable to naïve application (i.e., using the same categories and threshold values presented here) in a new area without some initial field-based evaluation.
4. *Quantified sediment-production factors* Finding appropriate numerical values to calibrate GLU production types of Low, Medium, and High can be challenging. Sespe Creek benefits from sediment sampling at the downstream gaging station to provide verification of our GLU predictions, rapid erosion rates that have required constructed debris basins to protect the downslope settlements, and long-term academic interest in its high rates of tectonic uplift so close to major population centers. However, we have been less confidently able to quantify rates of sediment production in other locations. The local data and the scientific

literature offers some justification for assuming order-of-magnitude differences in GLU production rates between the erosion processes associated with the GLU categories here, but equivalent differences may not apply everywhere (for instance, where overall rates of sediment production are lower).

Conclusions

The scientific literature suggests that discriminating watershed areas on the basis of lithology, hillslope gradient, and land cover in a singular climatic and tectonic domain should provide a basis to recognize relative rates of sediment production across a landscape. Extensive field observations applied in a 674-km^2 southern California watershed confirm this broad framework, with mass wasting and intense rilling and gullying common on steep, bare hillslopes underlain by weak, fine-grained sedimentary rocks; and progressively less rapid hillslope-erosion processes evident on progressively flatter, better vegetated, and/or stronger materials. Quantifying the average unit-area production of three broad categories of "GLUs" benefits from multiple decades of sediment-removal data from nearby debris basins, allowing a relatively low-precision but consistent accounting of both local and watershed-wide sediment yields, with unit-area rates that range from 200 to 25,000 t km^{-2} year^{-1}. Other data sources, namely geologically inferred uplift rates and suspended sediment measurements from the mainstem river, show that the Sespe Creek watershed is experiencing uplift of a few mm per year and is eroding at a modest fraction of that rate. Abundant relict fluvial landforms attest to the relative magnitudes of these two geologic processes. These results also broadly confirm the magnitude of aggregate sediment yield independently calculated from the GLU analysis and offer confidence for those applications where the spatial distribution of sediment sources and the potential for land-cover change are important parameters for management.

A "representative area" approach, typified here by the generation of GLUs to determine spatially explicit rates of sediment production, is useful for spatial extrapolation of sediment information to scales where sampling every point in the watershed is infeasible. The GLUs represent a quantifiable conceptual model of sediment production. GLUs can be used in their categorical form, for instance to highlight areas with disproportionately high unit-area sediment sources, or they can be calibrated with a numerical value to assist in developing a watershed sediment budget. Because the approach makes various simplifying assumptions based on (usually) limited and somewhat unreliable sediment data, GLUs are probably most appropriate as decadal-scale summaries of sediment production rates. However, many issues in environmental management depend on similar planning horizons: we have found the approach useful in a region where wildfires can create widespread changes in land cover, where urban development continues to encroach on once-natural areas, where fish habitat is largely structured by the availability of coarse sediment, and where the flood safety of downstream populations may depend on the effective management of sediment loads from their upstream watersheds. The approach thus permits the rapid visualization and application of geologic understanding about watershed sediment production, providing both a systematic framework for integrating geologic investigations and a planning tool for a range of social applications.

Acknowledgments Our thanks to colleagues with whom we discussed the development of this approach and who helped in the field: John Wooster, Jay Stallman, and Cliff Reibe. Rafael Real de Asua and Eric Panzer were instrumental in developing and executing the GIS analysis and in helping to draft the maps. The field work and much of the preliminary analysis were funded by the Ventura County Watershed Protection District in support of their assessment of post-fire flood risks to the town of Fillmore. Thanks also to the U.S. Forest Service–Ojai Ranger District office for granting access to all areas of the Los Padres National Forest for our field surveys, the U.S. Forest Service–Los Padres National Forest for sharing compiled geologic data and Day Fire spatial data, and Kevin Schmidt (USGS) for useful post-fire sediment production information from their ongoing study in the Day Fire area. Peter Wohlgemuth (USFS) reviewed a draft of the preliminary report for Ventura County, and shared valuable insights into sediment production and fire effects in this dynamic landscape. Our thanks also to the journal editors and two anonymous reviewers for careful and thoughtful evaluations.

References

Andrews ED, Antweiler RC (2012) Sediment fluxes from California coastal rivers: the influences of climate, geology, and topography. J Geol 120:349–366

Andrews E, Antweiler R, Neiman P, Ralph F (2004) Influence of ENSO on flood frequency along the California Coast. J Clim 17:337–348

Argus DF, Heflin MB, Donnellan A, Webb FH, Dong D, Hurst KJ, Jefferson DC, Lyzenga GA, Watkins MM, Zumberge JF (1999) Shortening and thickening of metropolitan Los Angeles measured and inferred by using geodesy. Geology 27:703–706

Beighley RE, Dunne T, Melack JM (2005) Understanding and modeling basin hydrology: interpreting the hydrological signature. Hydrol Process 19:1333–1353

Benda L, Dunne T (1997) Stochastic forcing of sediment supply to channel networks from landsliding and debris flow. Water Resour Res 33:2849–2863

Blythe AE, Burbank DW, Farley KA, Fielding EJ (2000) Structural and topographic evolution of the central Transverse Ranges, California, from apatite fissiontrack, (U/Th)/He and digital elevation model analyses. Basin Res 12:97–114

Booth DB, Dusterhoff SR, Stein ED, Bledsoe BP (2010) Hydromodification Screening Tools: GIS-based catchment analyses of potential changes in runoff and sediment discharge. Technical Report 605. Southern California Coastal Water Research Project.

Costa Mesa, CA. Available at ftp://sccwrp.org/pub/download/DOCUMENTS/TechnicalReports/605_HydromodScreeningTools_GIS_ES.pdf. Accessed 6 Nov 2013

Brownlie WR, Taylor BD (1981) Coastal sediment delivery by major rivers in Southern California. Sediment management of southern California mountains, coastal plains, and shorelines. Environmental Quality Laboratory Report 17-C, 314. Part C, California Institute of Technology, Pasadena

Buffington JM, Montgomery DR, Greenberg HM (2004) Basin-scale availability of salmonid spawning gravel as influenced by channel type and hydraulic roughness in mountain catchments. Can J Fish Aquat Sci 61:2085–2096

Burbank DW, Leland J, Fielding E, Anderson RS, Brozovic N, Reid-Mary R, Duncan C (1996) Bedrock incision, rock uplift and threshold hillslopes in the northwestern Himalayas. Nature 379:505–510

Cannon SH, Gartner JE, Wilson RC, Bowers JC, Laber JL (2008) Storm rainfall conditions for floods and debris flows from recently burned areas in southwestern Colorado and southern California. Geomorphology 96:250–269

Carson MA, Kirkby M (1972) Hillslope form and process. Cambridge University Press, London

Cayan D, Redmond K, Riddle L (1999) ENSO and hydrologic extremes in the western United States. J Climate 12:2881–2893

Çemen I (1989) Near-surface expression of the eastern part of the San Cayetano fault: a potentially active thrust fault in the California transverse ranges. J Geophys Res 94:9665–9677

Davis WM (1899) The geographical cycle. Geogr J 14:481–504

Dibblee T (1985a) Geologic map of the Old Man Mountain quadrangle, Ventura County, California. Scale 1:24,000. Dibblee Geological Foundation, Santa Barbara

Dibblee T (1985b) Geologic map of the Wheeler Springs quadrangle, Ventura County, California. Scale 1:24,000. Dibblee Geological Foundation, Santa Barbara

Dibblee T (1987) Geologic map of the Lion Canyon quadrangle, Ventura County, California. Scale 1:24,000. Dibblee Geological Foundation, Santa Barbara

Dibblee T (1990a) Geologic map of the Fillmore quadrangle, Ventura County, California. Scale 1:24,000. Dibblee Geological Foundation, Santa Barbara

Dibblee T (1990b) Geologic map of the Santa Paula Peak quadrangle, Ventura County, California. Scale 1:24,000. Dibblee Geological Foundation, Santa Barbara

Dibblee T (1996a) Geologic map of the Devils Heart Peak quadrangle, Ventura County, California. Scale 1:24,000. Dibblee Geological Foundation, Santa Barbara

Dibblee T (1996b) Geologic map of the Topatopa quadrangle, Ventura County, California. Scale 1:24,000. Dibblee Geological Foundation, Santa Barbara

Dietrich WE, Dunne T (1978) Sediment budget for a small catchment in mountainous terrain. Zeitschrift für Geomorphologie Supplementband 29:191–206

Dietrich WE, Bellugi DG, Sklar LS, Stock JD, Heimsath AM, Roering JJ (2003) Geomorphic transport laws for predicting landscape form and dynamics. In: Wilcock P, Iverson RM (eds) Prediction in geomorphology. American Geophysical Union, Washington DC, pp 103–132

Doerr SH, Shakesby RA, Walsh RPD (2000) Soil water repellency, its characteristics, causes and hydro-geomorphological consequences. Earth Sci Rev 51:33–65

Donnellan A, Hager BH, King RW (1993) Discrepancy between geological and geodetic deformation rates in the Ventura basin. Nature 366:333–336

Downs PW, Booth DB (2011) Geomorphology in environmental management. In: Gregory KJ, Goudie AS (eds) The sage handbook of geomorphology. Sage Publications Inc., Thousand Oaks, CA, pp 78–104

Downs PW, Gregory KJ (2004) River channel management: towards sustainable catchment hydrosystems. Oxford University Press, New York

Dunne T, Leopold LB (1978) Water in environmental planning. WH Freeman, San Francisco

Duvall A, Kirby E, Burbank D (2004) Tectonic and lithologic controls on bedrock channel profiles and processes in coastal California. J Geophys Res 109:F03002. doi:10.1029/2003JF000086

England CB, Holtan HN (1969) Geomorphic grouping of soils in watershed engineering. J Hydrol 7:217–225

England P, Molnar P (1990) Surface uplift, uplift of rocks, and exhumation of rocks. Geology 18:1173–1177

Farnsworth KL, Milliman JD (2003) Effects of climatic and anthropogenic change on small mountainous rivers: the Salinas River example. Glob Planet Change 39:53–64

Gabet EJ, Dunne T (2002) Landslides on coastal sage-scrub and grassland hillslopes in a severe El Niño winter: the effects of vegetation conversion on sediment delivery. Geol Soc Am Bull 114:983–990

Gabet EJ, Dunne T (2003) A stochastic sediment delivery model for a steep Mediterranean landscape. Water Resour Res 39:1237. doi:10.1029/2003WR002341

Gilbert GK (1904) Domes and dome structure of the High Sierra. Geol Soc Am Bull 15:29–36

Granger DE, Riebe CS (2007) Cosmogenic nuclides in weathering and erosion. In: Drvor JI (ed) Treatise on geochemistry, vol 5: surface and ground water, weathering, and soils. Elsevier, London

Gutowski VP (1978) Stream terraces along Sespe Creek, Ventura County, California. In: Fritsche AE (ed) Depositional environments of Tertiary rocks along Sespe Creek, Ventura County, California. Pacific Coast Paleogeography 3. Society of Economic Paleontologists and Mineralogists, pp 60–72

Heimsath AM (1998) The soil production function. Doctoral dissertation, University of California, Berkeley

Heimsath AM, Dietrich WE, Nishiizumi K, Finkel RC (1997) The soil production function and landscape equilibrium. Nature 388:358–361

Hicks D, Hill MJ, Shankar U (1996) Variation of suspended sediment yields around New Zealand: the relative importance of rainfall and geology. IAHS Publ Ser 236:149–156

Huftile GJ, Yeats RS (1995) Convergence rates across a displacement transfer zone in the western Transverse Ranges, Ventura basin, California. J Geophys Res 100:2043–2068

Inman DL, Jenkins SA (1999) Climate change and the episodicity of sediment flux of small California rivers. J Geol 107:251–270

Iwahashi J, Pike RJ (2007) Automated classifications of topography from DEMs by an unsupervised nested-means algorithm and a three-part geometric signature. Geomorphology 86:409–444

Kinnell PIA (2005) Why the universal soil loss equation and the revised version of it do not predict event erosion well. Hydrol Process 19:851–854

Kirchner JW, Finkel RC, Riebe CS, Granger DE, Clayton JL, Megahan WF (2001) Mountain erosion over 10 yr, 10 k.y., and 10 m.y. time scales. Geology 29:591–594

Lavé J, Burbank D (2004) Denudation processes and rates in the Transverse Ranges, southern California: erosional response of a transitional landscape to external and anthropogenic forcing. J Geophys Res 109:F01006. doi:10.1029/2003JF000023

Marshall ST, Cooke ML, Owen SE (2008) Effects of nonplanar fault topology and mechanical interaction on fault-slip distributions in the Ventura Basin, California. Bull Seismol Soc Am 98:1113–1127

McPhee J (1988) The control of nature: Los Angeles against the mountains. The New Yorker, New York

Meigs A, Yuleb D, Blythe AE, Burbank D (2003) Implications of distributed crustal deformation for exhumation in a portion of a transpressional plate boundary, Western Transverse Ranges, southern California. Quatern Int 101–102:169–177

Metcalf JG (1994) Morphology, chronology, and deformation of Pleistocene marine terraces, southwestern Santa Barbara County, California. Master's thesis, University of California, Santa Barbara

Milliman JD, Syvitski JPM (1992) Geomorphic/tectonic control of sediment discharge to the ocean: the importance of small mountain rivers. J Geol 100:525–544

Minear T, Kondolf GM (2009) Estimating reservoir sedimentation rates at large spatial and temporal scales: a case study of California. Water Resour Res. doi:10.1029/2007WR006703

Montgomery DR (1999) Process domains and the river continuum. J Am Water Resour Assoc 35:397–410

Moody JA, Smith JD (2005) Critical shear stress for erosion of cohesive soils subjected to temperatures typical of wildfires. J Geophys Res 110:F01004. doi:10.1029/2004JF000141

Orme AR (1998) Late Quaternary tectonism along the Pacific coast of the Californias: a contrast in style. In: Stewart RL, Vita-Finzi C (eds) Coastal tectonics, special publication 146. Geological Society, London, pp 179–197

Pelletier JD (2012) A spatially distributed model for the long-term suspended sediment discharge and delivery ratio of drainage basins. J Geophys Res 117:F02028. doi:10.1029/2011JF002129

Peterson MD, Bryant WA, Cramer CH, Cao T, Reichle M, Frankel AD, Lienkaemper JJ, McCrory MA, Schwartz DP (1996) Probabilistic seismic hazard assessment for the state of California. USGS Open-File Report 96–706

Peterson MD, Wesnousky SG (1994) Fault slip rates and earthquake histories for active faults in southern California. Bull Seismol Soc Am 84:1608–1649

Pinter N and Vestal WD (2005) El Niño-driven landsliding and postgrazing recovery, Santa Cruz Islands, California. J Geophys Res, 110, F2. doi:10.1029/2004JF000203

Portenga EW, Bierman PR (2011) Understanding Earth's eroding surface with ^{10}Be. GSA Today. doi:10.1130/G111A.1

Prosser IP, Williams L (1998) The effect of wildfire on runoff and erosion in native Eucalyptus forest. Hydrol Process 12:251–265

Ramos-Scharrón CE, MacDonald LH (2007) Development and application of a GIS-based sediment budget model. J Environ Manag 84:157–172

Reid LM, Dunne T (1996) Rapid construction of sediment budgets for drainage basins. Catena-Verlag, Cremlingen

Risse LM, Nearing MA, Nicks AD, Laflen JM (1993) Error assessment in the Universal Soil Loss Equation. Soil Sci Soc Am J 57:825–833

Rockwell TK (1988) Neotectonics of the San Cayetano fault, Transverse Ranges, California. Geol Soc Am Bull 100:500–513

Romans BW, Normark WR, McGann MM, Covault JA, Graham SA (2009) Holocene Santa Monica Basin, California: implications for evaluating source-to-sink flux at millennial time scales. Geol Soc Am Bull 121:1394–1408

Rowe PB, Countryman CM, Storey HC (1949) Probable peak discharges and erosion rates from Southern California watersheds as influenced by fire. US Forest Service report

Scott K, Williams RP (1978) Erosion and sediment yields in the Transverse Ranges, southern California. Geological Survey Professional Paper 1030

Selby MJ (1982) Hillslope materials and processes. Oxford University Press, New York

Shakesby RA, Doerr SH (2006) Wildfire as a hydrological and geomorphological agent. Earth Sci Rev 74:269–307

Spotila JA, House MA, Blythe AE, Niemi NA, Blank GC (2002) Controls on the erosion and geomorphic evolution of the San Bernardino and San Gabriel mountains, southern California. In: Barth A (ed) Contributions to crustal evolution of the southwestern United States. Special Paper 365. The Geological Society of America, Boulder, CO, pp 205–230

Trecker MA, Gurrola LD, Keller EA (1998) Oxygen-isotope correlation of marine terraces and uplift of the Mesa Hills, Santa Barbara, California, USA. Geol Soc Spec Publ 146:57–69

USDA NCSS (US Department of Agriculture, National Cooperative Soil Survey) (2012) Soil survey geographic (SSURGO) database

USFS (US Forest Service) (2006) 2006 Day Fire burned area emergency response (BAER) assessment. 2006 Day Fire Los Padres Portion Initial 2500-6, version 11-15-06

VCWPD (Ventura County Watershed Protection District) (2005) Debris and detention basins. Ventura, California

Walling DE, Webb BW (1983) Patterns of sediment yield. In: Gregory KJ (ed) Background to paleohydrology: Wiley, Chichester, pp 69–100

Warrick JA, Farnsworth KL (2009) Sources of sediment to the coastal waters of the Southern California Bight. In: Lee HJ, Normark WR (eds) Earth sciences in the urban ocean: the southern California continental borderland. Geological Society of America Special Paper 454, Boulder, CO, pp 39–52

Warrick JA, Mertes LAK (2009) Sediment yield from the tectonically active semiarid Western Transverse Ranges of California. Bull Geol Soc Am 121:1054–1070

Wells WG II (1981) Some effects of brushfires on erosion processes in coastal Southern California. In: Davies TRH, Pearse AJ (eds) Erosion and sediment transport in Pacific Rim Steeplands Symposium. Association of Hydrological Sciences, Christchurch, pp 305–342

Wells WG II (1987) The effects of fire on the generation of debris flows in southern California. Geol Soc Am Rev Eng Geol 7:105–114

Williams R (1979) Sediment discharge in the Santa Clara River basin, Ventura and Los Angeles counties, California. US Geological Survey, Menlo Park

Wills CJ, Weldon II RJ, Bryant WA (2008) Appendix A: California fault parameters for the National Seismic Hazard Maps and working group on California earthquake probabilities 2007. USGS Open File Report 2007–1437A

Wohlgemuth PM and Hubbert KR (2008) The effects of fire on soil hydrologic properties and sediment fluxes in chaparral steeplands, southern California. In: Narog MG (ed) Proceedings of the 2002 Fire Conference: managing fire and fuels in the remaining wildlands and open spaces of the southwestern United States. Gen. Tech. Rep. PSW-GTR-189. US Department of Agriculture, Forest Service, Pacific Research Station, Albany, pp 115–121